Title: Critical Parameters Dictating Efficiency of Membrane-mediated Drug Transfer using Nanoparticles

Saed Abbasi [†], *Kazuaki Kajimoto* [⊥] *and Hideyoshi Harashima* [†,] *,

[†] Faculty of Pharmaceutical Sciences, Hokkaido University, Kita 12, Nishi 6, Kita-ku, Sapporo, Hokkaido 060 0812, Japan

[⊥] Health Research Institute, National Institute of Advanced Industrial Science and Technology, 2217-14 Hayashi-cho, Takamatsu 761-0395, Kagawa, Japan

*Correspondence to:

Hideyoshi Harashima, Ph. D.

Laboratory for Molecular Design of Pharmaceutics

Faculty of Pharmaceutical Sciences, Hokkaido University

Kita 12 Nishi 6, Sapporo City, Hokkaido 060-0812, Japan

TEL: +81-11-706-3919

FAX: +81-11-706-4879

E-mail: harasima@pharm.hokudai.ac.jp

Abstract:

Curcumin, a low molecular weight, hydrophobic compound, exhibits strong anti-cancer effects and has a high margin of safety. However, its poor water solubility, rapid metabolism and degradation make it relatively ineffective, but intracellular delivery using nanoparticles (NPs) would solve these problems. In this study, we formulated curcumin in two-structurally distinct NPs: a nanoemulsion (Cur-NE) and a Niosome (Cur-NIO), evaluated their *in-vitro* cytotoxic effects and examined their mechanisms of drug delivery. The use of Cur-NIO resulted in an unexpected increase in the intracellular accumulation of curcumin and induced a potent cytotoxic effect compared to Cur-NE. To our surprise, however, the effects of the endocytosis of NIO as well as that for NE on the cellular delivery of curcumin were negligible. Consequently, we concluded that Cur-NIO delivers curcumin directly to the cytosol *via* transfer from the NIO to the cell membrane. The results of Förster resonance energy transfer (FRET) and phase-transfer studies indicate that Cur-NIO exhibits efficient transfer into model membranes or organic interfaces. Moreover, we found that Cur-NE shows a poor transfer efficiency. This could be due to the presence of a hydrophobic oil core that reduces the probability of curcumin to transfer upon contact with the membrane. To the best of our knowledge, this is the first study of the effect of NP structure on the membrane-mediated transfer efficiency of low molecular weight, hydrophobic compounds.

Key words:

Nanoemulsion, Niosome, Drug transfer, Drug release, Membranes, Drug Delivery, cytosolic delivery

Abbreviations:

Cur, Curcumin; DiD, 1,1′-dioctadecyl-3,3,3′,3′-tetramethylindodicarbocyanine; DOPE, 1,2-dioleoyl-sn-glycero-3-phosphoethanolamine; DOTAP, 1,2-dioleoyl-3-trimethylammonium-propane; EPC, egg phosphatidylcholine; FACS, fluorescence-activated cell sorting; FRET, Förster resonance energy transfer; NE, nanoemulsion; NIO, noisome; NP, nanoparticle; PEG, polyethylene glycol; T80, Tween 80.

Introduction

Design of nanoparticles (NPs) for the delivery of poorly water-soluble drugs has been long investigated. NPs can control the release rate of the drug and its pharmacokinetics and tissue distribution. In addition, NPs can control the intracellular trafficking and achieve drug targeting on a subcellular level (Cabral et al., 2018; Sato et al., 2017). Among the different modes of subcellular targeting, cytosolic delivery is sought after as it evades drug degradation in the harsh conditions of the lysosome and eventually results in superior drug efficacy. Multiple technologies have been developed for cytosolic delivery of macromolecules such as nucleic acids (Varkouhi et al., 2011), however, research on developing cytosolic delivery of poorly water-soluble small drugs is not very common.

Curcumin, the major active constituent of the spice turmeric, has attracted considerable interest throughout the last couple of decades as a promising therapy for cancer and inflammatory disorders (Anand et al., 2008; Elias et al., 2016). However, shortcomings arising from various physicochemical characteristics of this compound such as poor aqueous solubility, rapid chemical degradation and enzymatic metabolism have impeded its clinical application (Anand et al., 2007). A recent report by Nelson et al (2017) spotted light on the failure of

curcumin in clinical trials, despite of the extensive research. This emphasizes the need of clinically translatable NPs for the efficient delivery of hydrophobic small drug such as curcumin. . Wide range of formulations such as polymeric micelles, nanoemulsions and liposomes have been reported to enhance the performance of curcumin both *in-vitro* and *in-vivo*, yet the exact mechanism of drug delivery by most of the curcumin-loaded NPs is not fully clear (Steuber et al., 2016; Lin et al., 2012; Pengying et al., 2017).

In this study, we initially formulated curcumin in the form of a nanoemulsion (Cur-NE) since it is easy to prepare, economical to use and known to efficiently incorporate lipophilic drugs (Abbasi et al., 2016). However, the cytotoxicity activity of Cur-NE against a human cervical cancer cell line (Hela cells) *in-vitro* was weak. Unexpectedly, conventional methodology that is commonly used to enhance the potency of drug-loaded NPs by boosting their endocytosis were unsuccessful in terms of enhancing the potency of Cur-NE (Khalil et al., 2006). As an alternative approach, we formulated curcumin in the form of a structurally-distinct NP i.e. a noisomal preparation (Cur-NIO), which is vesicular particle composed of nonionic surfactants (Mandal et al., 2013). Interestingly, NIO improved the potency of curcumin compared to NE and free curcumin, which cannot be explained by conventional reasoning.

Thereafter, we performed a comparison between curcumin-loaded NE and NIO and elucidated their mechanisms of action. The findings resulted in the discovery of an unconventional and potent cytosolic drug delivery strategy for curcumin that involves membrane-mediated drug transfer using the NIO. Our findings provide new insights that would be clearly of interest concerning research on the delivery of labile small-drugs, which are readily enzymatically metabolized or unstable at the acidic pH of the lysosome, to construct new classes of potent NPs that deliver drugs directly into the cytosol through the cell membrane.

Materials and methods

1. Materials

Coconut oil, PEG600, Tween 80 (T80), cholesterol and 2-deoxy-D-glucose were purchased from Sigma-Aldrich (St. Louis, MO). Egg phosphatidylcholine (EPC) was obtained from NOF (Tokyo, Japan). Sodium Azide, Curcumin, Dulbecco's Modified Eagle's Medium (DMEM), Dimethyl sulfoxide (DMSO) and Diisopropyl ether were obtained from Wako Chemicals (Osaka, Japan). The 1,1′-dioctadecyl-3,3,3′,3′-tetramethylindodicarbocyanine (DiD) fluoresce Probe was supplied by Thermo Fisher Scientific (Waltham, MA), and both NBD-DOPE and Rhodamine-DOPE were purchased from Avanti Polar Lipids (Alabaster, Al). A Cell Counting Kit-8 was obtained from Dojindo (Kumamoto, Japan) and RC Dialysis membrane (MWCO 12-14 kD) from Spectrum Laboratories (Rancho Dominguez, CA). Monolein and Triolein were purchased from Kanto chemicals and TCI, Respectively (Tokyo, Japan).

2. Measurement of curcumin solubility

Excess amount of curcumin powder was added into a definite amount of material, such as double distilled water, oils and surfactants and stirred at 800 rpm and room temperature (RT) for 7hrs. The mixture was then left to equilibrate overnight and the supernatant was centrifuged twice (15000 xg, RT) to remove any undissolved curcumin. The supernatant was dissolved and diluted in DMSO and the concentration of curcumin was determined using a spectrophotometer (Beckman Coulter, Brea, CA, USA) at λ=434.

3. Preparation of curcumin-loaded Nanoemulsion and Niosome

For the preparation of curcumin-loaded Nanoemulsion (Cur-NE), curcumin was dissolved in a mixture of T80 and coconut oil and vigorously mixed prior to the addition of the

aqueous phase. The aqueous phase was comprised of a buffer system (HEPES, 10 mM, pH 7.4) and EPC as a surfactant. The mixture was then vortexed and sonicated using a probe-type sonicator (Misonix, Farmingdale, NY) for 6 min. The total conc. of NE was 101.4 mg/ml and the weight ratio of curcumin: T80: Coconut oil: EPC was 1.4: 39.4: 54.2: 4.9, respectively.

A curcumin-loaded Niosome (Cur-NIO) was prepared by the film-hydration method. Briefly, 0.11 mg Curcumin, 1.97 mg T80 and 0.29 mg cholesterol (weigh ratio equivalent to 4.6: 83: 12.2, respectively) were dissolved in chloroform in a glass tube. The organic phase was removed by evaporation and the resulting film was hydrated using 1ml of pre-heated HEPES buffer. Probe sonication was applied for 6 min to form nano-sized niosomal particles. Finally, the noisome suspension was centrifuged at 5000 g for 3 min at RT to remove large particles and free surfactants. For labeling of the NPs with fluorescent probes, the probes were dissolved with the NP components and prepared using the same procedures.

4. Characterization of Cur-NE and Cur-NIO

Particle size, polydispersity index, and ζ-potential were measured using a Malvern Zetasizer (Malvern Instruments, Malvern, UK). Encapsulation efficiency (EE %), a measure of the ability of the nanoparticulate system to retain curcumin in the particle phase, was estimated by centrifuging the Cur-NE and Cur-NIO at 15000 g for 5 min. The amount of insoluble curcumin in the form of precipitated crystals or powder was quantified using a spectrophotometer. Since no precipitation of curcumin was detected upon centrifuging the samples, the EE % was taken to be 100%. Drug loading (DL) was calculated using the following formula:

$$\mathrm{DL} = \frac{\text{Wt. of curcumin}}{\text{Wt. of curcumin} + \text{Wt. of all components}} * 100\%$$

Transmission Electron Microscope (TEM) images were obtained using a Hitachi HD2000 scanning TEM (Tokyo, Japan). Cur-NE and Cur-NIO were mounted on a copper grid. Lipids were stained with 1% phosphotungstic acid and allowed to dry completely prior to the observations (Vacc=200kV Mag=x250k).

5. *In-vitro* cytotoxicity assay

Human cervical cancer cell line (Hela cells) were cultured in DMEM supplemented with 10% FBS ((+) DMEM) for 24 hrs (37 ºC, 5% CO_2) in 96 well plates at a density of 0.5×10^4 cell/ well. Free curcumin (10 mM stock in DMSO), curcumin-loaded NE and NIO and empty counterparts were serially diluted in (+) DMEM and applied to cells in a dose dependent manner. After the treatment, the plates were further incubated for 24 hours and a cell viability assay (water-soluble tetrazolium salt) was then carried out. The absorbance was measured using a microplate reader (Perkin Elmer, Waltham, MA) and the relative cell viability was calculated as the ratio of absorbance of the treated wells to the non-treated ones.

6. confocal microscopy observation

Hela cells ($2x\ 10^5$) were seeded in glass-base dishes and incubated for 24 hrs (37 ºC, 5% CO2). Treatment with 50 µM curcumin of either the free form (0.5% v/v DMSO), or the Cur-NE/NIO was then applied to cells and incubated for 3 hrs at 4 ºC or 37 ºC in (+) DMEM. The NPs were also labeled with DiD (2 mol% of the curcumin content).. 3 ul of Heochest (1 mg/ml) was added to each dish 10 minutes before the end of the incubation period to stain the nucleus. Dishes were washed twice with cold (+) DMEM and once with phenol-free culture media. Finally, a 2ml aliquot of the phenol-free culture media was added and the dishes were observed by confocal laser microscopy (Nikon, Tokyo, Japan).

7. Quantitative assessment of cellular uptake

Hela cells (2x 10^5) were seeded in 6-well culture plates and incubated for 24 hrs (37 ºC, 5% CO_2) prior to the treatment. The cells were incubated with 50 µM curcumin of either the free form (0.5% v/v DMSO) and DiD-labeled Cur-NE/NIO (2 mol% of the curcumin content) for 3 hrs at 37 ºC or 4 ºC in (+) DMEM. When the cells were incubated for 24 hrs prior to evaluation of cellular uptake, the curcumin concentration was 30 or 10 µM to allow observation of fluorescence signals from viable cells (0.3% or 0.1% v/v DMSO, respectively, in case of free curcumin). For ATP depletion, 10 mM Sodium Azide and 50 mM 2-deoxy-D-glucose were applied 1 hr prior the treatment and kept until the end of the incubation period. The cells were washed 3 times with cold Phosphate Buffer Saline (PBS), trypsinized and collected by centrifugation (1800 g, 3 mins, 4 ºC). The pellet was washed one more time with cold PBS and suspended in PBS containing 0.5% bovine serum albumin and 0.1% Sodium Azide, and analyzed using a FACS Calibur flow cytometer (BD Biosciences, San Jose, CA).

8. *In-vitro* drug release

Cur-NE and Cur-NIO were dialyzed individually against 45 ml of a release buffer consisting of 20 % v/v ethanol and 0.4% w/v T80. Samples were incubated at 37 ºC under constant rotation in a dark chamber. At various time points, 10 ml of the release media was withdrawn and replaced with fresh media to maintain sink conditions. The concentration of curcumin was determined by its absorbance at λ=428 nm using a spectrophotometer, and the cumulative release was calculated using the following equation:

$$\mathrm{Qn} = \mathrm{CnV}_{\circ} \sum_{\mathrm{i}=0}^{\mathrm{n}-1} \mathrm{CiVi}$$

$$\text{Cumulative release } \% = \frac{\text{Qn}}{\text{Total curcumin amount}} * 100\%$$

Where Q_n represents the amount of released curcumin at time= n, C_n is the Curcumin concconcentration of in the release media,V_0 is the volume of release media, C_i is the concentration at that time and V_i is the volume of the withdrawn sample (10ml).

9. FRET studies

The extent of curcumin transfer into cells by a membrane-mediated mechanism was estimated using the Förster resonance energy transfer (FRET) principle. NIO or NE containing 15 uM Curcumin as a donor probe and 15 uM Rho-DOPE as the acceptor probe were prepared. Each NP was diluted 5 times in a liposomal suspension composed of 1.5 mM EPC and 0.5 mM cholesterol, as a cell membrane mimic. At various time points, a sample was withdrawn and its fluorescence intensity (FI) spectrum recorded after excitation at 424-428 nm. The FRET ratios for NIO and NE were calculated as (FI 496 / FI 496 + FI 586) or (FI 494 / FI 494 + FI 586), respectively. The FRET ratio after diluting the NIO or NE 5 times with HEPES buffer represents the lowest value (No transfer), while the maximal transfer was assumed to occur when the FRET between probes is canceled. This was achieved by disrupting the NIO or NE upon a 5 fold dilution in 10% Triton. As a control, a phospholipid based non-transferable pair of probes, ie, NBD-DOPE and Rho-DOPE, was added to either the NIO or NE. Samples were excited at 476 nm and FRET ratios were computed as FI 532/ (FI 532+ FI 588). Representative spectra of FRET pairs in buffer, liposomal suspensions and in Triton are provided in **supplementary Figure 1.**

The % Transfer was calculated as follows:

$$\%\text{Transferred} = \frac{\text{FRET}_t - \text{FRET}_0}{\text{FRET}_{max} - \text{FRET}_0}$$

Where FRET_t represents the FRET ratio at a definite time point, FRET_0 is the minimal value (diluted in HEPES buffer), FRET_{max} is the maximum value (diluted in 10% Triton).

10. Phase transfer studies

100 ul of Cur-NE or Cur-NIO that contain equivalent amounts of curcumin was added to 900 ul of Diisopropyl ether and allowed to rotate continuously at 4 rpm. At various time points, 300 ul portions of of diisopropyl ether were withdrawn and replaced with fresh Diisopropyl ether. The withdrawn sample was evaporated to dryness and the remaining curcumin was dissolved in DMSO and its absorption was measured at λ=434 nm. Cumulative release % was calculated as described above.

11. Statistical analysis

The statistical significance between two groups was analyzed using unpaired, two tailed student's t test. For multiple comparisons between 3 or more groups, ANOVA followed by SNK test was performed. A statistically significant difference was set at $p \leq 0.05$.

Results and discussion

1. A nanoemulsion as a carrier for curcumin

Curcumin is classified as class 2 according to the biopharmaceutical classification system (Wan et al., 2012), meaning it is water insoluble but membrane permeable. Such poor aqueous solubility limits the use of free curcumin as a therapeutic agent. In this study, a bottom-up design approach was adapted for the formulation of curcumin-loaded NPs. A preliminary screening of the saturated solubility of curcumin in different materials, such as oils and

surfactants, was carried out to select the materials showing high affinity to curcumin. Tween 80 (T80), a non-ionic surfactant composed of polyethylene glycol (PEG) as the hydrophilic head and an oleic acid ester as the hydrophobic tail, could substantially dissolve curcumin compared to water or coconut oil. (81.7 ± 6.7, 0.0005 ± 0.0003 and 2.44 ± 0.24 mg/ml, respectively), **Supplementary Table 1**. This could be attributed to the hydrogen bonding between the methoxy groups of PEG of T80 and the hydroxyl moieties of curcumin (Sharma and Pathak, 2016). To confirm this, the solubility of curcumin in PEG600 solvent was compared to that in triolein or monoolein. Triolein is a glycerol esterified with 3 oleic acid molecules and monoolein is esterified to only 1 oleic acid. Both compounds are used because they are structurally similar to the oleic acid ester of T80. It was found that curcumin is much more soluble in PEG600 (126.5 ± 4.5 mg/ml) compared to either triolein or monoolein (0.59 ± 0.09 and 3.1 ± 0.1 mg/ml, respectively), **Supplementary Table 1**, indicating that curcumin mostly binds the PEG part of T80, but not the hydrophobic tail.

T80, as a principal solvent of curcumin and a surfactant, was used to formulate a curcumin-loaded nanoemulstion (Cur-NE) as an initial step. Unfortunately, Cur-NE showed a low efficiency in delivering curcumin to Hela cells compared to free curcumin solubilized by DMSO (**Figure 1A**), which was also less potent than free curcumin in the reduction of cell viability (**Figure 2A**). In an attempt to further enhance the uptake of curcumin using NE, 2.5 mg/ml DOTAP (N-[1-(2,3-Dioleoyloxy)propyl]-N,N,N-trimethylammonium), a cationic lipid that is commonly used to promote the endocytosis of NPs[13], was added to the Cur-NE, which resulted in an increase in the ζ-potential to +17.5 mV. However, surprisingly, although the uptake of DiD (a label for NE particles) was elevated after the addition of DOTAP (**Figure 1B**),

the signal of curcumin inside the cells remained unchanged (**Figure 1A**). This is because the curcumin-bound NE ends up in the lysosome, where curcumin might get deactivated.

2. ***Niosome enhances the uptake and potency of curcumin***

After failing to increase the accumulation of active curcumin inside the cells by enhancing the endocytosis of NE, it became clear an alternative strategy was needed to enhance the uptake and potency of curcumin. Using T80 as the principal solvent for curcumin, a structurally-distinct type of NP was constructed by hydrating a dried film composed of curcumin, T80 and cholesterol. This NP is a niosomal vesicle (Cur-NIO), with a particle size comparable to that of Cur-NE, **Table 1** and **Figure 3**.

Surprisingly, the Cur-NIO showed a more potent cytotoxic effect than either Cur-NE and free curcumin (in DMSO), **Figure 2A**, which is consistent with the FACS result showing that the cellular accumulation of curcumin in the Cur-NIO treated group is higher compared to free Cur after 24 hr of incubation (**Supplementary Figure 2).** The EC_{50} of Cur-NIO, Free curcumin and Cur-NE were determined to be 14, 34 and 70 uM, respectively. Given that curcumin is mainly soluble in T80, and that T80 comprises the main surface component in both NPs, the substantial difference in potencies between NE and NIO was quite unexpected, and this prompted us to conduct a comparative analysis to elucidate their mechanism responsible for the delivery of this drug. It is also noteworthy that neither the Empty-NE nor the Empty-NIO showed any substantial toxicity to Hela cells when applied at same concentrations of the curcumin-loaded counterparts (**Figure 2B**).

3. Endocytosis doesn't contribute in the uptake of curcumin from NE or NIO

In general, NPs exert their action by either one or both of the following modes: the release of drugs in the extracellular region, followed by the cellular uptake of the free drug, or the release of the encapsulated drugs inside the cell after particle endocytosis (Allen and Cullis, 2004). To clarify which of these mechanisms are applicable for each NP, the effect of endocytosis on the uptake of curcumin and a marker (DiD) was carried out in initial experiments. The native fluorescence of curcumin was used to monitor its uptake (Ghosh and Ryan, 2014; Wu et al, 2017), and DiD, a charged and highly hydrophobic florescent probe that is membrane impermeable, was used to probe the uptake of the NP itself. When the NPs were incubated at 37 ºC, both green and red signals were observed inside the cells, indicating the uptake of both curcumin and the NPs, respectively (**Figure 4A**). The curcumin signal inside the cells was stronger in the case of cur-NIO compared to Cur-NE, indicating that a higher cellular accumulation of curcumin results in a higher cell killing activity, as observed in **Figure 2A**. A quantitative assessment of fluorescence intensity was performed using FACS and the findings are shown in **supplementary Figure 3**. Considering only the uptake data at 37 ºC, it could be mistakenly concluded that a higher uptake of particles (DiD) resulted in a higher delivery of curcumin in the case of the Cur-NIO treatment. However, and surprisingly, curcumin accumulated inside the cells, even when endocytosis was diminished at 4 ºC, **Figure 4B and supplementary Figure 3**.. Furthermore, it is noteworthy that the superior uptake of curcumin from the NIO was maintained irrespective of whether or not endocytosis was inhibited. This is particularly evident when we calculated the ratio of curcumin-to-DiD geo means measured by FACS (**Supplementary Figure 3)**. The Curcumin/DiD ratio after treatment using NIO at 37 ºC was 2.2 folds higher than that of the NE. Likewise, the ratio was 2.3 folds higher in favor of NIO

when incubated at 4 ºC, suggesting that the intracellular delivery of curcumin from either the NE or NIO was independent of the endocytosis of NPs.

Stronger evidence was obtained when the cellular uptake of curcumin and DiD was compared with or without ATP depletion using 50 mM 2-deoxy-D-glucose and 10 mM Sodium Azide, as shown in **Figure 5**. Similarly, the DiD signal was almost completely diminished after endocytosis was inhibited in ATP-depleted conditions, while the cellular uptake of curcumin continued to take place. The slight increase in curcumin's uptake signal after ATP depletion observed in **Figure 5** could be due to the higher uptake of the released curcumin by passive diffusion. This could be attributed to the increase in cell membrane area available for diffusion as a result of detachment of some of the cells in the ATP-depleted group.

Collectively, the failure of DOTAP to enhance the intracellular accumulation of active curcumin and the observation of significant curcumin accumulation inside the cells, despite the inhibition of endocytosis, confirm that endocytosis makes a negligible contribution to the delivery of active curcumin by NE or NIO. This could be explained by the fact that curcumin is readily enzymatically metabolized and the resulting metabolites are much different from the parent compound (Heger et al., 2014). Therefore, it is not surprising that the endocytosed curcumin along with the NP ends in the lysosome where curcumin is metabolized and loses its fluorescence and activity. Coinciding with our findings, Fotticchia et al. (2017) showed that curcumin is more pharmacologically active when localized in the cytosol rather the endosome/lysosome, which suggest the presence of a degradative for curcumin in the lysosome.

4. ***Extracellular release as a delivery mechanism of NE but not NIO***

As discussed above, NPs could also release their cargos outside the cells into culture media, followed by the cellular uptake of the free drug. Curcumin is membrane permeable, meaning it can enter cells by passive diffusion after being released from the NP (Wan et al., 2012). The extracellular release kinetics of drugs are usually estimated by *in-vitro* techniques such as the dialysis cassette (Modi and Anderson, 2013), which provides an estimation of the rate of release of a drug under sink conditions. As shown in **Figure 6**, an approximate 50% release occurred after a solution of Cur-NE was dialyzed for 24 hrs. This slow and sustained release of cur-NE explains its weak cytotoxic effect as observed in **Figure 2A.** Likewise, Cur-NIO showed a sustained release that is a little bit faster (66% release after 24 hrs), **Figure 6**. Given that Cur-NIO exhibits a slow *in-vitro* release, and most importantly, bearing in mind that the uptake of released curcumin cannot exceed that of free curcumin (solubilized by DMSO), the potent cytotoxic effect and the higher uptake of curcumin from the Cur-NIO compared to free curcumin (**Figure 2A and Supplementary Figure 2, respectively**) cannot be explained exclusively by extracellular release.

5. Membrane-mediated drug transfer as a delivery mechanism of NIO

At this point, it could be safely concluded that the mechanism for the delivery of curcumin from Cur-NE involves the extracellular release of curcumin into the culture media, which is a slow process that renders Cur-NE less potent. On the other hand, the mechanism of delivery of the Cur-NIO cannot be explained by either endocytosis or the extracellular release of curcumin. Therefore, we hypothesized that Cur-NIO induces its action through an unconventional drug delivery mechanism that involves the direct and efficient delivery of curcumin into the cytosol through the plasma membrane (Kim et al., 2009), **Figure 7**. In other terms, we proposed a model

in which a substantial amount of curcumin is transferred into the cell upon contact between the niosomal membrane and the cell membrane.

To test the abovementioned hypothesis, we evaluated the kinetics of release of curcumin under true sink conditions i.e. in the presence of a hydrophobic membrane pool (Shabbits et al., 2002). The extent of curcumin transfer in the presence of cell membranes was estimated using a FRET principle, in which a double labeled NIO was mixed with a liposomal suspension mimicking the plasma membrane. First, curcumin, the donor, and Rhodamine –DOPE, the acceptor, were loaded in the NIO. For FRET to occur, donor and acceptor probes must be in reasonably close proximity to each other and oriented in a manner that favors energy transfer (Zou et al., 2013; Li et al., 2018). When the Cur-Rho NIO was in a buffer system, no change in the fluorescence spectrum was observed and thus, the % Transferred at 0 min was calculated to be 0%.On the other hand, when Cur-Rho NIO was diluted in Triton solution, the FRET spectrum was substantially changed, indicating the disruption of the NIO and the loss of energy transfer between the probes. Although the fluorescence intensity peak of Rho-DOPE did not decline to 0 after mixing with Triton, **Supplementary Figure 1**, this spectrum was postulated as 100% Transfer. This is because the remaining peak of Rho-DOPE is due to its emission when excited at 424 nm, as evidence by the presence of emission peak 550-600 nm when the fluorescence spectrum of Rho-DOPE was recorded as a single component (data not shown).Once the Cur-Rho NIO was diluted in a liposomal suspension, a very rapid release occurred in the first minute that rapidly became saturated, **Figure 8A.** Compared to its control, or the NBD-Rho NIO, curcumin showed a much larger degree of transfer which confirms the highly diffusive nature of curcumin upon mixing the noisome with membranes. The control consisted of a pair of phospholipid-anchored probes, NBD and Rhodamine-DOPE, to represent a non-transferrable system, since the

transfer of phospholipids between membranes at low concentrations is very slow or even negligible (Wimley and Thompson, 1991; Wirtz, 1974). Nonetheless, the small increase in transfer observed in NBD-Rho NIO could be attributed to a minor reduction in FRET efficiency as a result of the combined effect of the transfer of probes, the disruption of NIO or fusion between the NIO and the liposomal membrane. This modest disruption/fusion of the NIO in the presence of liposomes should be addressed carefully in future studies when we consider the *in-vivo* application of our system, since this could also predict particle instability in biological systems. A possible strategy is to modify the surface of the NIO with trigger-responsive polymer coatings, that protect the NIO in blood/gastric fluids until removed upon arrival to the target tissue. Nonetheless, it is also interesting to note that the % of curcumin transferred from the Cur-Rho NIO compared to its control, **Figure 8A**, was more significant compared to the transfer of curcumin from Cur-Rho NE compared to its control, **Figure 8B**. In other terms, the superior cellular uptake of curcumin and the more potent cytotoxic effect of Cur-NIO compared to Cur-NE could be explained by the fact that NIO delivers curcumin by the membrane-mediated transfer mechanism more efficiently.

To further elaborate the mechanism responsible for such membrane-mediated release, we designed a specific phase-transfer experiment in which the release of curcumin from NIO was compared to that from NE. In this experiment, NPs diluted in an aqueous buffer were mixed with diisopropyl ether as an organic phase. Since the two phases are immiscible, and T80, which makes up the major solvent of curcumin and confers a hydrophilic surface to the NPs, is not soluble in diisopropyl ether, transfer of curcumin-loaded NPs themselves from the aqueous phase into the organic phase is excluded. Therefore, the release of curcumin was assumed to occur solely at the interface between the water and diisopropyl ether **Figure 8C**. Cur-NIO showed

larger transfer of curcumin compared to that for Cur-NE, **Figure 8D**, which further supports the conclusion that curcumin is transferred more efficiently from the NIO in the presence of lipophilic acceptor compartments such as the cell membrane.

6. The mechanism of membrane-mediated transfer

The exact mechanism responsible for curcumin transfer is currently not clear, but there are two main possibilities for a hydrophobic molecule to be released in the presence of a nanoacceptor (such as a cell membrane or a liposome): either to be released into water followed by diffusion into the nanoacceptor, which is a process governed by fick's diffusion and is referred to as short-distance release in water (Wang et al, 2010), or by direct transfer upon contact between the nanocarrier and the nanoacceptor phases, which is caused by particle collision driven by Brownian motion (Chen et al., 2008). We propose that the latter as the mechanism for the membrane-mediated transfer of curcumin from Cur-NIO for two main reasons: the first is because curcumin is believed to be located on the surface of the NPs due to its high affinity to the PEG moieties of T80. Second, the PEG on the surface of the NPs causes membranes to come into very close contact by lowering the activity of adjacent water molecules (Ahkong et al., 1987). This explanation is compatible with Chen et al., (2008), who confirmed the rapid transfer of hydrophobic probes loaded in PEG-PDLLA micelles upon mixing with model membranes. Taken together, a situation in which curcumin is localized on the NIO surface and a PEG layer that forces close contact between the NIO and the acceptor membranes is present, curcumin would be expected to transfer mainly *via* collision and contact.

7. Why is Cur-NIO a more efficient membrane-mediated drug transfer species compared to Cur-NE?

The question that is yet to be addressed is why Cur-NIO exhibits a more efficient membrane-mediated drug transfer compared to Cur-NE, given that both NPs have comparable sizes and are composed of T80; the main surface component and the principal solvent of curcumin. One possibility is that the difference in transfer efficiency is due to the difference in drug loading (DL), **Table 1**. When we compare 2 structurally-distinct NPs, there are 3 dependent formulation factors we need to consider: particle size, overall DL (indexed by the weight of curcumin to the total weight of the NP) and cur/T80 density (an index of curcumin loading in the main solvent). If we wish to fix both of DL and cur/T80 density for the sake of comparison, particle size will change as the oil/surfactant ratio of the NE will change as well. Here, we evaluated the effect of cur/T80 density with fixed particle size on curcumin uptake. In fact, the cur/T80 density is more accurate than overall DL in estimating the effect of drug loading on drug release and transfer kinetics, as T80 represent the main curcumin-dissolving component (**Supplementary Table 1**). In this study, the weight density of the cur/T80 was around 1.5-fold higher in case of Cur-NIO compared to Cur-NE. Hence, it is possible that the higher density resulted in a higher rate of transfer into the cell membrane. However, when a pair of Cur-NE and NIO was prepared that have the same Cur/T80 weight density (5.4 %) and the uptake of curcumin by Hela cells was evaluated using FACS, the superiority of curcumin uptake from Cur-NIO was preserved, **Figure 9A**. This indicates that efficient intracellular delivery of curcumin using the NIO is not dependent on curcumin loading ratio in T80. We are still curious to know the effect of overall DL on the membrane-mediated transfer of curcumin, which could be experimentally tackled in future studies. However, and interestingly, Loew S et al (2011) developed a theoretical model for the estimation of release/transfer kinetics of poorly water-soluble drugs between liposomes. Their model involved 2 mechanisms of release: diffusion and

collision. Diffusion represents the release of drug molecules from donor to acceptor liposomes through the aqueous phase, while collision represents the direct transfer between liposomal membranes. Their model showed that DL is dependent on the diffusion mechanism but not the collision. In other words, high DL increase the rate constant of drug release in aqueous phases but doesn't affect the membrane-mediated transfer. Therefore, there must be an alternate critical factor that affects the difference in transfer efficiency between Cur-NE and NIO.

In some cases, molecules behave differently when formulated on a nanoscale compared to their status in bulk materials. In other words, even if curcumin is believed to be associated with the PEG moieties of T80 through hydrogen bond interactions, the supramolecular arrangement of T80 and coconut oil in the form of a core-shell nanostructure might provide curcumin with additional hydrophobic environment when in the NE form. Such an environment would permit curcumin to be located deeper from the outermost surface, thus reducing its interaction with water, **Figure 9B**. On the contrary, the lack of a hydrophobic core in the case of NIO would leave curcumin molecules to be more exposed to the surface and more susceptible to transfer upon contact with membranes or interfaces, **Figure 9B**. To confirm this hypothesis, fluorescence spectra of Cur-NE and Cur-NIO having the same curcumin concentrations were obtained after excitation at 424 nm. Interestingly, the spectrum of Cur-NE showed a greater intensity and exhibited a 12-nm blue shift compared to Cur-NIO, **Figure 9 C and D respectively**, indicating that curcumin is located in a less polar microenvironment away from water when formulated in NE. This observation is consistent with the effect of curcumin inclusion in the hydrophobic pockets of albumin or cyclodextrin, as reported previously (Yang et al., 2013; Moussa et al., 2016). Further investigations will be needed to characterize the nature of the bonding and interactions between T80, coconut oil and curcumin at the surface of NE.

Nonetheless, this is the first report to establish a connection between the structure of the NP and its efficiency in transferring small hydrophobic molecules such as curcumin.

Conclusion

We performed mechanistic comparisons between curcumin-loaded NE and NIO and elucidated their mechanisms of drug delivery, and report on an efficient strategy for delivering curcumin using a niosomal nanoparticle, which involves the direct transfer of curcumin into the cytosol *via* a membrane-mediated transfer mechanism. Furthermore, we addressed the critical factors that are necessary for a NP to exhibit efficient membrane-mediated drug transfer. We propose that the Cur-NIO efficiently transfers curcumin due to the lack of a hydrophobic core, which renders curcumin molecules exposed to the surface and susceptible to transfer upon contact with a membrane.

Acknowledgment

This manuscript was supported by the Special Education and Research Expenses of the Ministry of Education, Culture, Sports, Science and Technology of Japan. The authors thank Dr. M. S. Feather for the language polishing.

Supporting Information

Quantitative evaluation of cellular uptake of curcumin and DiD label by FACS analysis; Representative fluorescence spectra of FRET analysis; Saturated solubility of curcumin in various materials

References

Abbasi S, Kajimoto K, Harashima H. (2016). Elimination of the biphasic pharmacodynamics of 15d-PGJ2 by controlling its release from a nanoemulsion. International Journal of Nanomedicine, 8(11), 2685–94. https://doi.org/10.2147/IJN.S106297

Ahkong QF, Desmazes JP, Georgescauld D, Lucy JA (1987) Movements of fluorescent probes in the mechanism of cell fusion induced by poly (ethylene glycol). J Cell Sci 88:389–398.

Allen, T. M. (2004). Drug Delivery Systems: Entering the Mainstream. Science, 303(5665), 1818–1822. https://doi.org/10.1126/science.1095833

Anand, P., Kunnumakkara, A. B., Newman, R. A., & Aggarwal, B. B. (2007). Bioavailability of Curcumin: Problems and Promises. Molecular Pharmaceutics, 4(6), 807–818. https://doi.org/10.1021/mp700113r

Anand, P., Sundaram, C., Jhurani, S., Kunnumakkara, A. B., & Aggarwal, B. B. (2008). Curcumin and cancer: An "old-age" disease with an "age-old" solution. Cancer Letters, 267(1), 133–164. https://doi.org/10.1016/j.canlet.2008.03.025

Cabral, H., Miyata, K., Osada, K., & Kataoka, K. (2018). Block Copolymer Micelles in Nanomedicine Applications. Chemical Reviews, 118(14), 6844–6892. https://doi.org/10.1021/acs.chemrev.8b00199

Chen, H., Kim, S., Li, L., Wang, S., Park, K., & Cheng, J.-X. (2008). Release of hydrophobic molecules from polymer micelles into cell membranes revealed by Forster resonance energy transfer imaging. Proceedings of the National Academy of Sciences, 105(18), 6596–6601. https://doi.org/10.1073/pnas.0707046105

Elias, G.; Jacob, P. J.; Hareeshbabu, E.; Mathew, V. B.; Krishnan, B.; Krishnakumar, K. Curcumin: Transforming the spice to a wonder drug. Int. J. Pharm. Sci. Res. 6 (2015) 2671−2680.

Fotticchia, T., Vecchione, R., Scognamiglio, P. L., Guarnieri, D., Calcagno, V., Di Natale, C., … Netti, P. A. (2017). Enhanced Drug Delivery into Cell Cytosol via Glycoprotein H-Derived Peptide Conjugated Nanoemulsions. ACS Nano, 11(10), 9802–9813. https://doi.org/10.1021/acsnano.7b03058

Ghosh, M., & Ryan, R. O. (2014). ApoE enhances nanodisk-mediated curcumin delivery to glioblastoma multiforme cells. Nanomedicine, 9(6), 763–771. https://doi.org/10.2217/nnm.13.35

Heger, M., van Golen, R. F., Broekgaarden, M., & Michel, M. C. (2013). The Molecular Basis for the Pharmacokinetics and Pharmacodynamics of Curcumin and Its Metabolites in Relation to Cancer. Pharmacological Reviews, 66(1), 222–307. https://doi.org/10.1124/pr.110.004044

Khalil, I. A. (2006). Uptake Pathways and Subsequent Intracellular Trafficking in Nonviral Gene Delivery. Pharmacological Reviews, 58(1), 32–45. https://doi.org/10.1124/pr.58.1.8

Kim, C. K., Ghosh, P., Pagliuca, C., Zhu, Z.-J., Menichetti, S., & Rotello, V. M. (2009). Entrapment of Hydrophobic Drugs in Nanoparticle Monolayers with Efficient Release into Cancer Cells. Journal of the American Chemical Society, 131(4), 1360–1361. https://doi.org/10.1021/ja808137c

Kim, T. W., Kim, Y. J., Chung, H., Kwon, I. C., Sung, H. C., & Jeong, S. Y. (2002). The role of non-ionic surfactants on cationic lipid mediated gene transfer. Journal of Controlled Release, 82(2–3), 455–465. https://doi.org/10.1016/s0168-3659(02)00138-4

Li, D., Zhuang, J., Yang, Y., Wang, D., Yang, J., He, H., … Qi, J. (2018). Loss of integrity of doxorubicin liposomes during transcellular transportation evidenced by fluorescence resonance energy transfer effect. Colloids and Surfaces B: Biointerfaces, 171, 224–232. https://doi.org/10.1016/j.colsurfb.2018.07.022

Lin, Y.-L., Liu, Y.-K., Tsai, N.-M., Hsieh, J.-H., Chen, C.-H., Lin, C.-M., & Liao, K.-W. (2012). A Lipo-PEG-PEI complex for encapsulating curcumin that enhances its antitumor effects on curcumin-sensitive and curcumin-resistance cells. Nanomedicine: Nanotechnology, Biology and Medicine, 8(3), 318–327. https://doi.org/10.1016/j.nano.2011.06.011

Loew, S., Fahr, A., & May, S. (2011). Modeling the Release Kinetics of Poorly Water-Soluble Drug Molecules from Liposomal Nanocarriers. Journal of Drug Delivery, 2011, 1–10. https://doi.org/10.1155/2011/376548

Mandal, S., Banerjee, C., Ghosh, S., Kuchlyan, J., & Sarkar, N. (2013). Modulation of the Photophysical Properties of Curcumin in Nonionic Surfactant (Tween-20) Forming Micelles and Niosomes: A Comparative Study of Different Microenvironments. The Journal of Physical Chemistry B, 117(23), 6957–6968. https://doi.org/10.1021/jp403724g

Modi, S., & Anderson, B. D. (2013). Determination of Drug Release Kinetics from Nanoparticles: Overcoming Pitfalls of the Dynamic Dialysis Method. Molecular Pharmaceutics, 10(8), 3076–3089. https://doi.org/10.1021/mp400154a

Moussa, Z., Hmadeh, M., Abiad, M. G., Dib, O. H., & Patra, D. (2016). Encapsulation of curcumin in cyclodextrin-metal organic frameworks: Dissociation of loaded CD-MOFs enhances stability of curcumin. Food Chemistry, 212, 485–494. https://doi.org/10.1016/j.foodchem.2016.06.013

Nelson, K. M., Dahlin, J. L., Bisson, J., Graham, J., Pauli, G. F., & Walters, M. A. (2017). The Essential Medicinal Chemistry of Curcumin. Journal of Medicinal Chemistry, 60(5), 1620–1637. https://doi.org/10.1021/acs.jmedchem.6b00975

Sato, Y., Sakurai, Y., Kajimoto, K., Nakamura, T., Yamada, Y., Akita, H., & Harashima, H. (2016). Innovative Technologies in Nanomedicines: From Passive Targeting to Active Targeting/From Controlled Pharmacokinetics to Controlled Intracellular Pharmacokinetics. Macromolecular Bioscience, 17(1), 1600179. https://doi.org/10.1002/mabi.201600179

Shabbits, J.A., Chiu, G.N.C., Mayer, L.D. (2002). Development of an in vitro drug release assay that accurately predicts in vivo drug retention for liposome-based delivery systems, J. Control. Release, 84, 161–170. https://doi.org/10.1016/S0168-3659(02)00294-8

Sharma, V., & Pathak, K. (2016). Effect of hydrogen bond formation/replacement on solubility characteristics, gastric permeation and pharmacokinetics of curcumin by application of powder solution technology. Acta Pharmaceutica Sinica B, 6(6), 600–613. https://doi.org/10.1016/j.apsb.2016.05.015

Steuber, N., Vo, K., Wadhwa, R., Birch, J., Iacoban, P., Chavez, P., & Elbayoumi, T. (2016). Tocotrienol Nanoemulsion Platform of Curcumin Elicit Elevated Apoptosis and Augmentation of Anticancer Efficacy against Breast and Ovarian Carcinomas. International Journal of Molecular Sciences, 17(11), 1792. https://doi.org/10.3390/ijms17111792

Varkouhi, A. K., Scholte, M., Storm, G., & Haisma, H. J. (2011). Endosomal escape pathways for delivery of biologicals. Journal of Controlled Release, 151(3), 220–228. https://doi.org/10.1016/j.jconrel.2010.11.004

Wan, S., Sun, Y., Qi, X., & Tan, F. (2011). Improved Bioavailability of Poorly Water-Soluble Drug Curcumin in Cellulose Acetate Solid Dispersion. AAPS PharmSciTech, 13(1), 159–166. https://doi.org/10.1208/s12249-011-9732-9

Wang, H., Xu, J., Wang, J., Chen, T., Wang, Y., Tan, Y. W., … Chen, H. (2010). Probing the Kinetics of Short-Distance Drug Release from Nanocarriers to Nanoacceptors. Angewandte Chemie International Edition, 49(45), 8426–8430. https://doi.org/10.1002/anie.201001065

Wimley, W. C., & Thompson, T. E. (1991). Phosphatidylethanolamine enhances the concentration-dependent exchange of phospholipids between bilayers. Biochemistry, 30(17), 4200–4204. https://doi.org/10.1021/bi00231a014

Wirtz, K. W. A. (1974) TRANSFER OF PHOSPHOLIPIDS BETWEEN MEMBRANES. Biochimica et Biophysica Acta, 344 95-117. https://doi.org/10.1016/0304-4157(74)90001-X

Wu, P., Jia, Y., Qu, F., Sun, Y., Wang, P., Zhang, K., … Wang, X. (2017). Ultrasound-Responsive Polymeric Micelles for Sonoporation-Assisted Site-Specific Therapeutic Action. ACS Applied Materials & Interfaces, 9(31), 25706–25716. https://doi.org/10.1021/acsami.7b05469

Wu, P., Jia, Y., Qu, F., Sun, Y., Wang, P., Zhang, K., … Wang, X. (2017). Ultrasound-Responsive Polymeric Micelles for Sonoporation-Assisted Site-Specific Therapeutic Action. ACS Applied Materials & Interfaces, 9(31), 25706–25716. https://doi.org/10.1021/acsami.7b05469

Yang, M., Wu, Y., Li, J., Zhou, H., & Wang, X. (2013). Binding of Curcumin with Bovine Serum Albumin in the Presence of ι-Carrageenan and Implications on the Stability and

Antioxidant Activity of Curcumin. Journal of Agricultural and Food Chemistry, 61(29), 7150–7155. https://doi.org/10.1021/jf401827x

Zou, P., Chen, H., Paholak, H. J., & Sun, D. (2013). Noninvasive Fluorescence Resonance Energy Transfer Imaging of in Vivo Premature Drug Release from Polymeric Nanoparticles. Molecular Pharmaceutics, 10(11), 4185–4194. https://doi.org/10.1021/mp4002393

Figure legends

Figure 1. Effect of modifying Cur-NE with DOTAP on (A) curcumin and (B) DiD cellular uptake. 30 uM free curcumin (DMSO), DiD-labeled Cur-NE and DOTAP-Cur-NE were incubated with Hela cells for 24 hrs at 37 ºC in (+) DMEM prior to FACS analysis.

Figure 2. *In-vitro* cytotoxicity of (A) Free curcumin and Cur-loaded NPs. (B) Empty NPs. Formulations were incubated for 24 hrs with Hela cells in (+) DMEM prior to evaluating cell viability. Empty NE and NIO were applied in concentrations corresponding to the curcumin-loaded counterparts. Data represent the mean ± SD (n=3).

Figure 3. Size characterization of Cur-loaded NPs. **(A)** Transmission electron microscopy (TEM) images of Cur-NE and **(B)** Cur-NIO. **(C)** Size distribution curves of Cur-NE and Cur-NIO obtained using dynamic light scattering.

Figure 4. Cellular uptake of curcumin and DiD, as evaluated by confocal microscopy after incubation at (A) 37 ºC and (B) 4 ºC. Hela cells were incubated for 3 hrs in (+) DMEM post treatment with 50 uM curcumin and 1 uM DiD. Scale bar: 50 um.

Figure 5. **Cellular uptake of curcumin and DiD using FACS analysis in ATP-depleted and non-depleted conditions**. **(A)** Uptake of curcumin. **(B)** Uptake of DiD. Cells were incubated at 37 ºC for 3 hrs in (+) DMEM post treatment with 50 uM curcumin and 1 uM DiD. Data represent mean ± SD (n=3).

Figure 6. ***In-vitro*** **release of curcumin from Cur-NE and Cur-NIO, as measured using a dialysis procedure.** Data represent the mean ± SD (n=3). *$p<0.05$.

Figure 7. Proposed mechanisms of curcumin delivery by NE and NIO. While the endocytosis of curcumin-loaded NE or NIO does not contribute to any substantial cellular accumulation of active curcumin, extracellular release remains as the main delivery mechanism for Cur-NE. On the other hand, neither endocytosis nor extracellular release explain the potent cytotoxic effect of Cur-NIO, and therefore, we propose that Cur-NIO delivers its load *via* a membrane-mediated transfer mechanism.

Figure 8. **Evaluation of the membrane-mediated transfer of curcumin**. **(A)** Transfer of curcumin from Cur-Rho NIO upon dilution in a liposomal suspension compared to NBD-Rho NIO as a control for low transfer efficiency. **(B)** Transfer of curcumin from Cur-Rho NE upon dilution in a liposomal suspension compared to NBD-Rho NE as a control for low transfer

efficiency. **(C)** Scheme of the phase-transfer model in which curcumin is transferred into the organic phase through the water-organic solvent interface. **(D)** Transfer of curcumin into the diisopropyl ether phase from Cur-NE and Cur-NIO. Data represent the mean ± SD (n=3). *p<0.05. **p<0.01. ns: not significant.

Figure 9. Factors dictating efficiency of curcumin transfer from NPs (A) Uptake of curcumin by Hela cells after treatment using Cur-NE and Cur-NIO having the same Cur/T80 density. Cells were incubated for 3 hrs post treatment at 37 ºC with 50 uM curcumin. Data represent the mean ± SD (n=4-5), *p<0.05. **(B)** Illustration showing the hypothesized difference in localization of curcumin on the surface of the NIO or NE. Curcumin is hypothesized to locate in deeper regions on the surface of the NE due to hydrophobic interaction with the coconut oil core, while curcumin is expected to be located on the outermost layer of the NIO. **(C)** Fluorescence intensity spectra of Cur-NE and Cur-NIO containing the same curcumin concentration. **(D)** Normalized spectra showing the blue shift of Cur-NE.

Tables

Table 1. Characterization of Cur-NE and Cur-NIO

	Size (nm)	**PDI**	**ζ-potential (mV)**	**DL (wt%)**
Cur-NE	130 ± 18	0.18 ± 0.03	-7.2 ± 0.6	1.34 ± 0.04
Cur-NIO	142 ± 13	0.09 ± 0.03	-15 ± 1.9	4.49% ± 0.05

Data represent the mean ± SD (n=3-4).

Figures

Figure 1

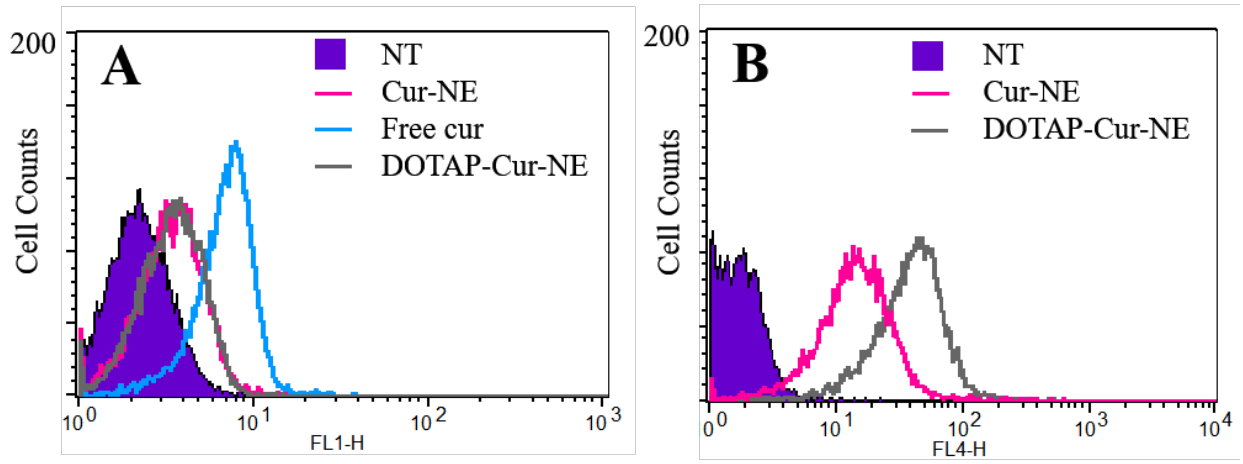

Figure 2

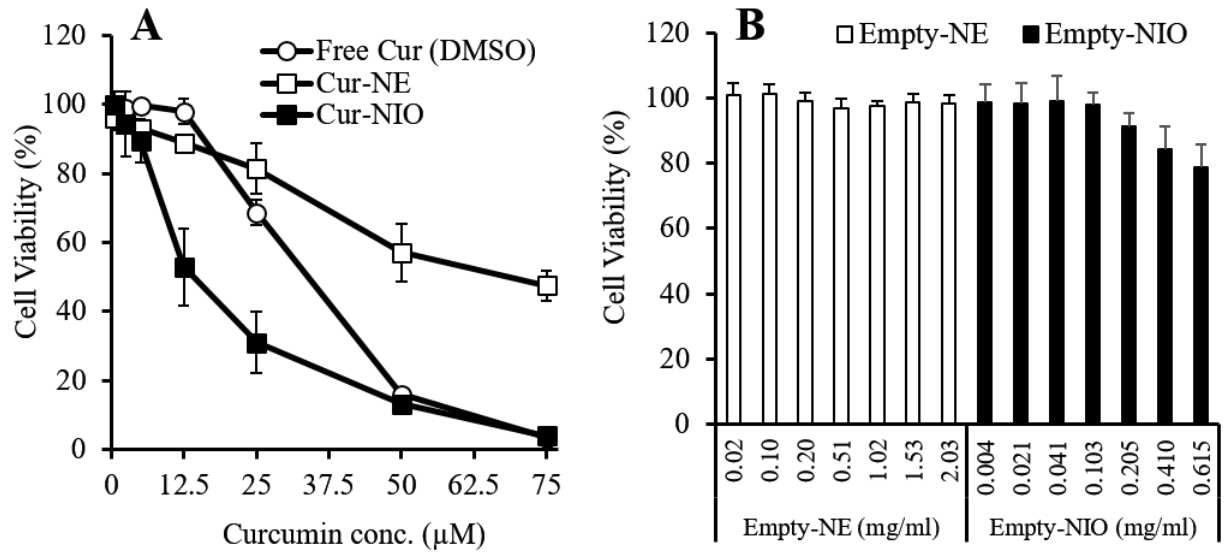
A
Free Cur (DMSO)
Cur-NE
Cur-NIO
Cell Viability (%)
120
100
80
60
40
20
0
0
12.5
25
37.5
50
62.5
75
Curcumin conc. (μM)
B
Empty-NE
Empty-NIO
Cell Viability (%)
120
100
80
60
40
20
0
0.02
0.10
0.20
0.51
1.02
1.53
2.03
0.004
0.021
0.041
0.103
0.205
0.410
0.615
Empty-NE (mg/ml)
Empty-NIO (mg/ml)

Figure 3

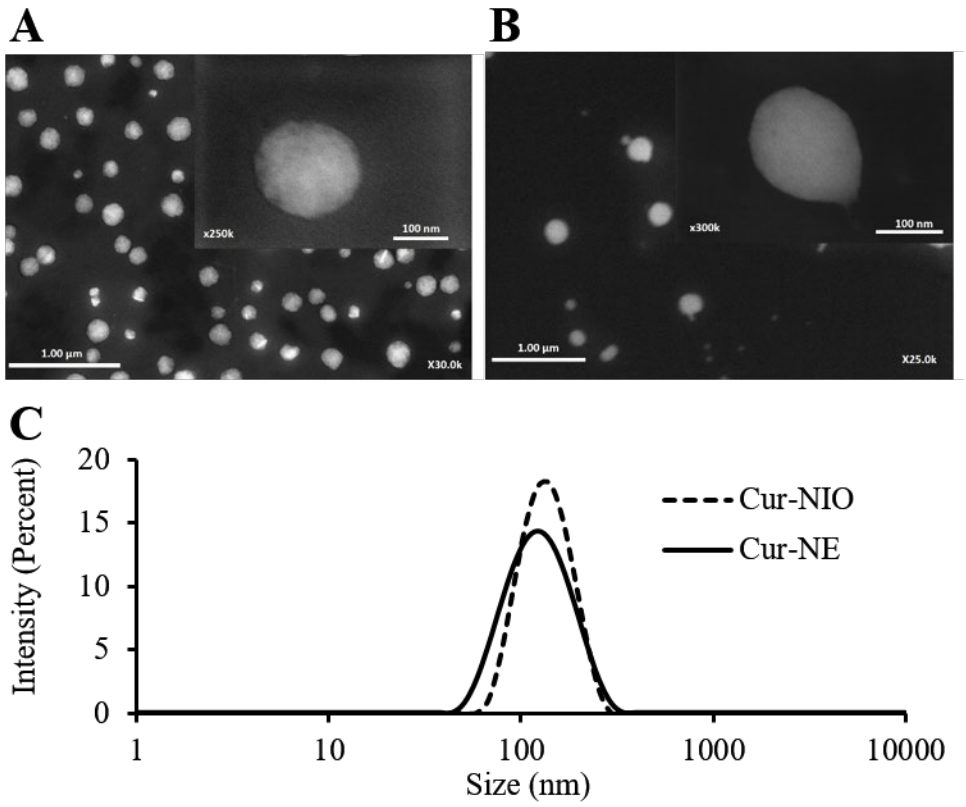
A
B
x250k
100 nm
1.00 µm
X30.0k
x300k
100 nm
1.00 µm
X25.0k
C
Intensity (Percent)
20
15
10
5
0
1
10
100
1000
10000
Size (nm)
Cur-NIO
Cur-NE

Figure 4

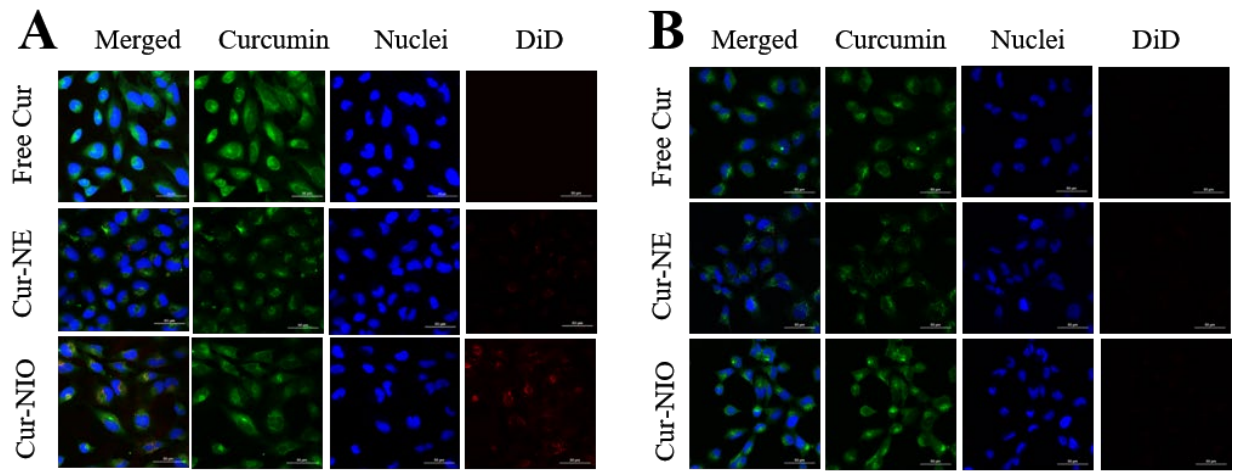
A
Merged
Curcumin
Nuclei
DiD
Free Cur
Cur-NE
Cur-NIO
B
Merged
Curcumin
Nuclei
DiD
Free Cur
Cur-NE
Cur-NIO

Figure 5

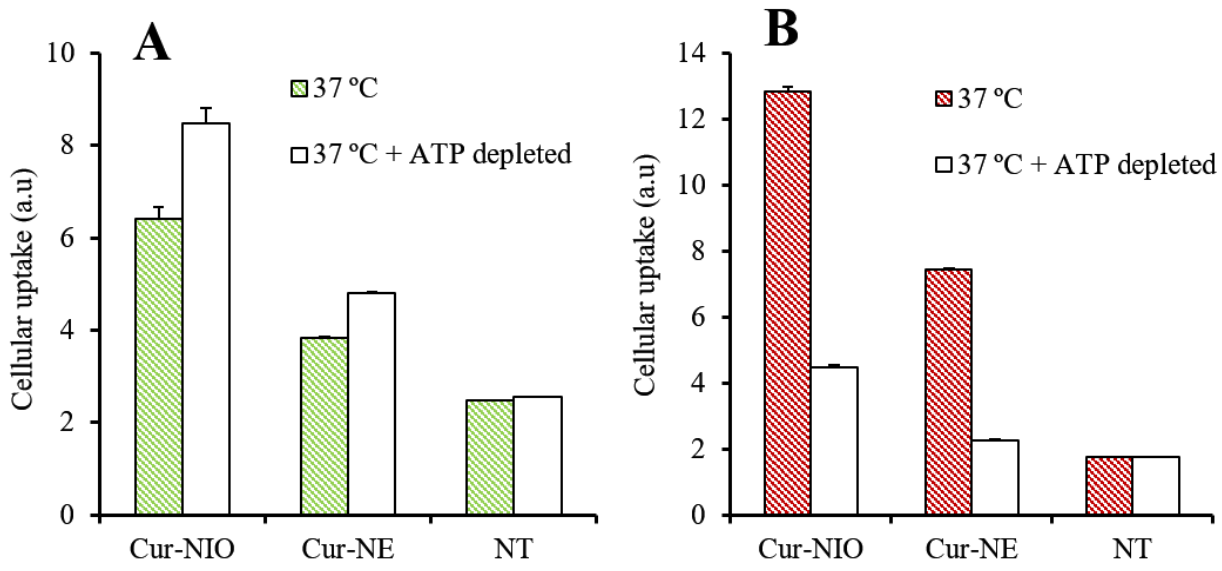
A
37 ºC
37 ºC + ATP depleted
Cellular uptake (a.u)
0
2
4
6
8
10
Cur-NIO
Cur-NE
NT
B
37 ºC
37 ºC + ATP depleted
Cellular uptake (a.u)
0
2
4
6
8
10
12
14
Cur-NIO
Cur-NE
NT

Figure 6

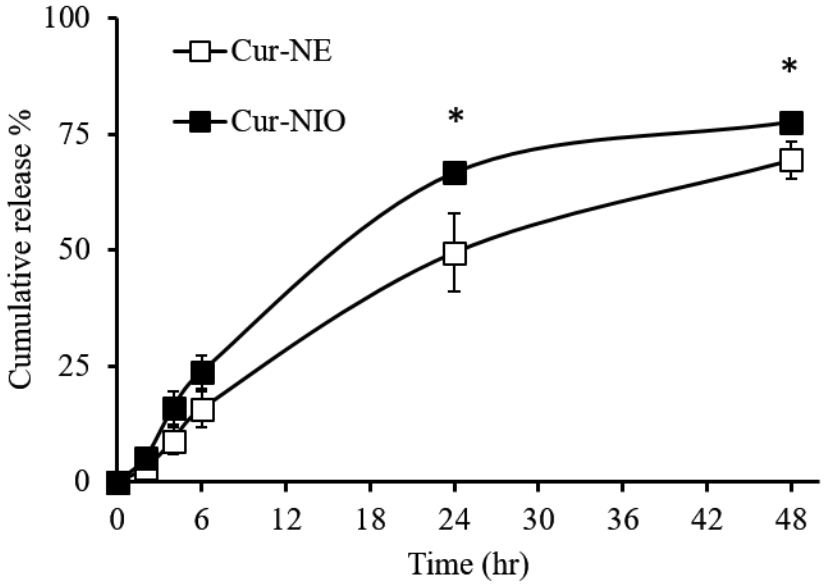
100
75
50
25
0
Cumulative release %
Cur-NE
Cur-NIO
*
*
0
6
12
18
24
30
36
42
48
Time (hr)

Figure 7

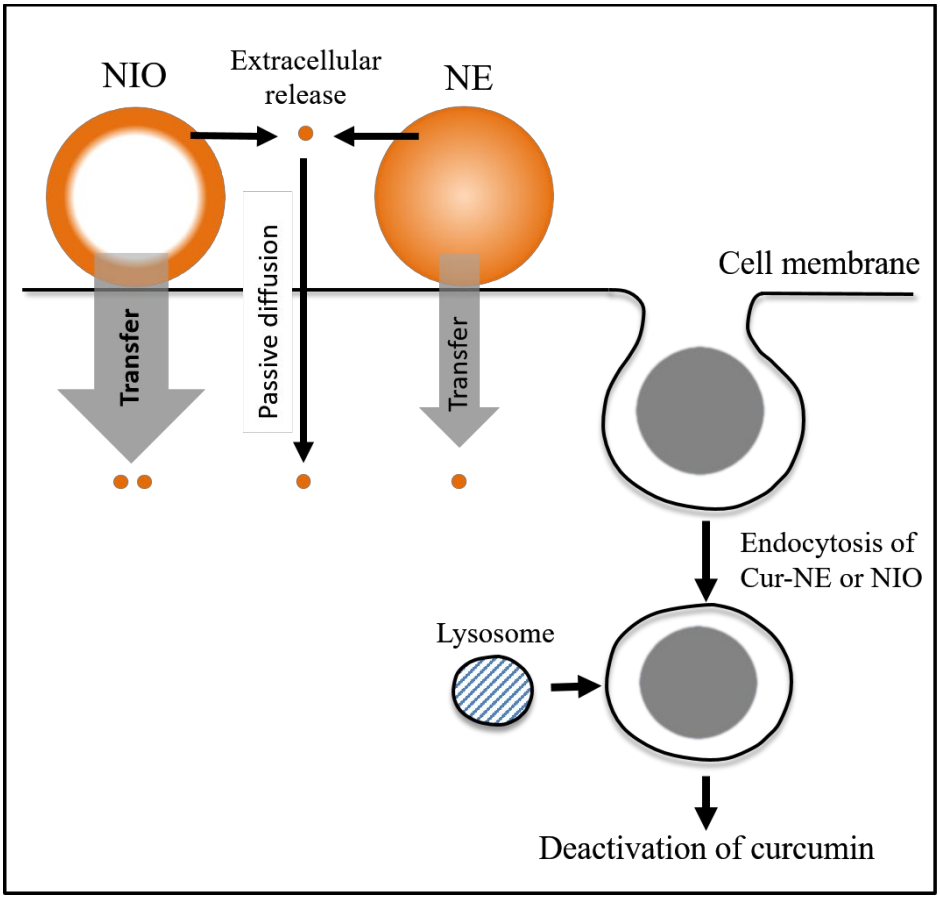
NIO
Extracellular release
NE
Transfer
Passive diffusion
Transfer
Cell membrane
Endocytosis of Cur-NE or NIO
Lysosome
Deactivation of curcumin

Figure 8

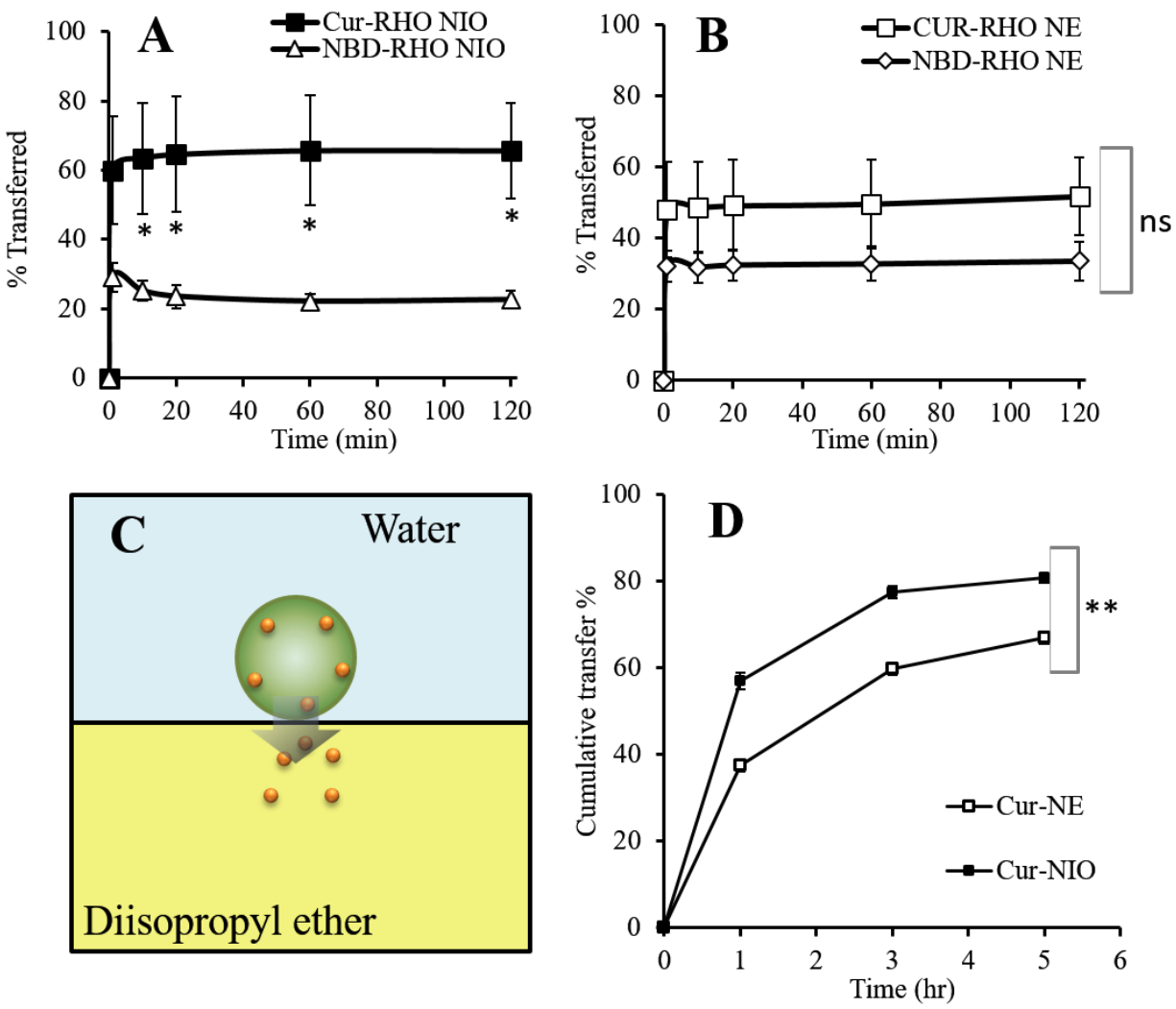
A
Cur-RHO NIO
NBD-RHO NIO
% Transferred
Time (min)
B
CUR-RHO NE
NBD-RHO NE
ns
C
Water
Diisopropyl ether
D
Cumulative transfer %
Time (hr)
Cur-NE
Cur-NIO
**

Figure 9

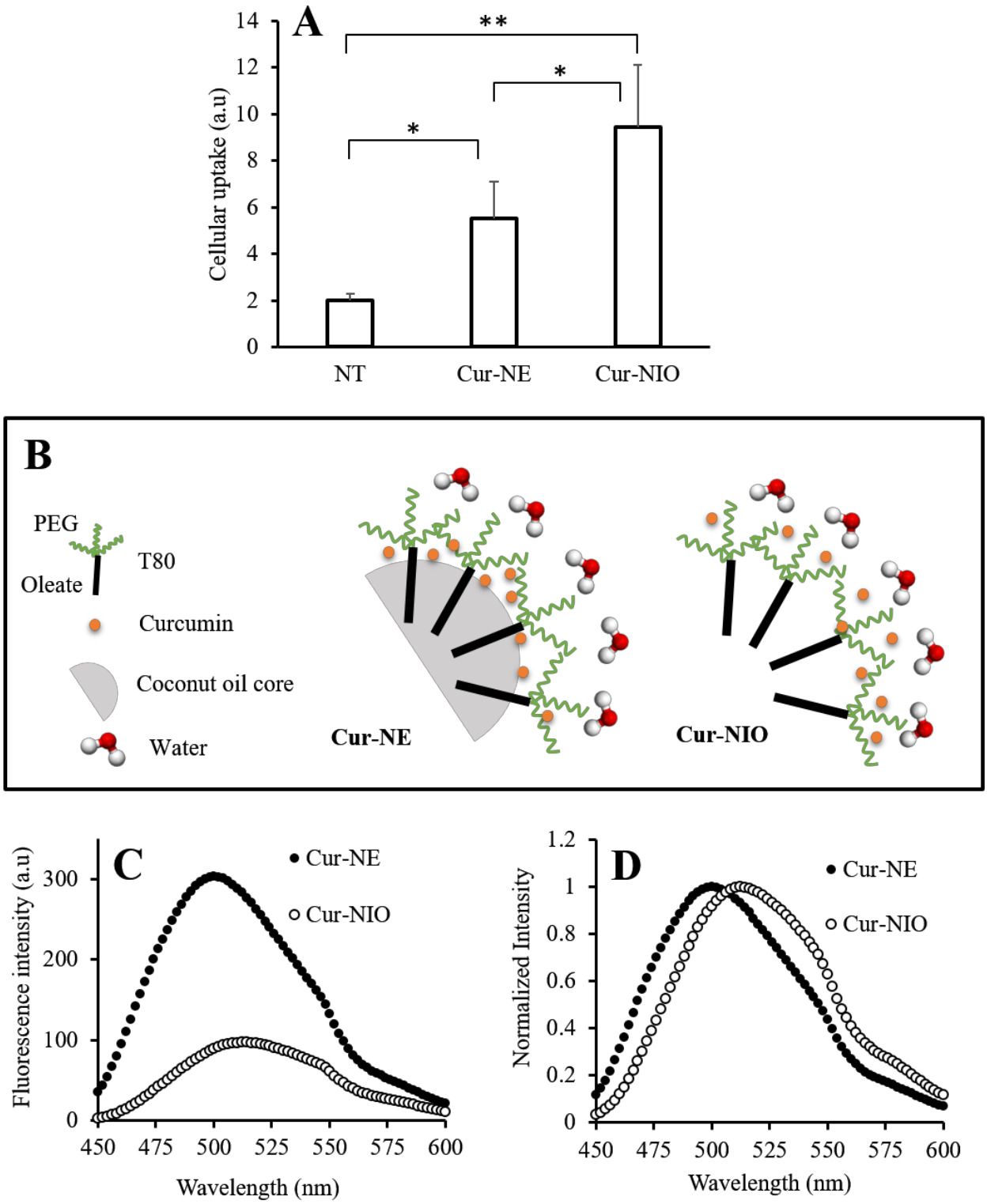
A
Cellular uptake (a.u)
14
12
10
8
6
4
2
0
**
*
*
NT
Cur-NE
Cur-NIO
B
PEG
T80
Oleate
Curcumin
Coconut oil core
Water
Cur-NE
Cur-NIO
C
Fluorescence intensity (a.u)
300
200
100
0
Cur-NE
Cur-NIO
450
475
500
525
550
575
600
Wavelength (nm)
D
Normalized Intensity
1.2
1
0.8
0.6
0.4
0.2
0
Cur-NE
Cur-NIO
450
475
500
525
550
575
600
Wavelength (nm)